

# CMOS Differential and Amplified Dosimeter with Field Oxide N-Channel MOSFETs

S. Carbonetto, *Student Member, IEEE*, M. Garcia-Inza, *Member, IEEE*, J. Lipovetzky, *Member, IEEE*, M. J. Carra, *Student Member, IEEE*, E. Redin, L. Sambuco Salomone, and A. Faigón

**Abstract**—We propose the use of a CMOS differential circuit with inherent amplification to enhance the performance of n-channel field oxide MOSFETs as ionizing radiation dosimeters. These new dosimeters are aimed to be used in low dose applications such as X-ray diagnosis. The circuit is presented and described, and a discrete-level prototype was tested as regards sensitivity, temperature variations compensation and signal-to-noise ratio at different operation conditions. Results show that, comparing to a single MOSFET dosimeter, on chip amplification is possible along with temperature induced error attenuation. The highest sensitivity measured with respect to  $\gamma$  radiation was 0.4 V/rad. The circuit successfully measured the dose delivered in an X-ray image diagnosis environment with a sensitivity of approximately 0.5 V/rad.

**Index Terms**—Dosimeters, MOS devices, radiation effects, solid-state detectors.

## I. INTRODUCTION

METAL–OXIDE–SEMICONDUCTOR (MOS) dosimeters are field effect transistors (FETs), generally p-channel type, where the shift in the threshold voltage ( $V_T$ ) is used to measure absorbed dose [1], [2]. When the sensor is exposed to radiation fields, ionization occurs within the gate oxide, and holes are likely to be captured in oxide traps near the interface with the semiconductor [3], [4]. This positive charge build-up (PCB) is mainly responsible for the  $V_T$  shifts.

Low dose dosimetry, as involved in X-ray diagnosis or personnel dosimetry, is still today challenging for MOS radiation sensors. The sensitivities required to achieve such a low dose resolution are not easily met with standard MOS dosimeters. Historically, thick gate oxide devices were used when high sensitivity dosimeters were needed. These type of dosimeters are

Manuscript received July 11, 2014; revised September 24, 2014; accepted November 02, 2014. Date of publication November 27, 2014; date of current version December 11, 2014. This work was supported by ANPCyT and UBA by Grants PICT Redes 2007 1907 and UBACyT Y064. The work of S. Carbonetto was supported by a Peruilh grant.

S. Carbonetto, M. Garcia-Inza, M. J. Carrá, E. Redin, and L. Sambuco Salomone are with the Device Physics-Microelectronics Lab., INTECIN, Facultad de Ingeniería, Universidad de Buenos Aires, C1063ACV, Ciudad de Buenos Aires, Argentina. (e-mail: scarbonetto@fi.uba.ar; magarcia@fi.uba.ar; mcarra@fi.uba.ar; eredin@fi.uba.ar; lsambuco@fi.uba.ar)

J. Lipovetzky and A. Faigón are with the Device Physics-Microelectronics Lab., INTECIN, Facultad de Ingeniería, Universidad de Buenos Aires, C1063ACV, Ciudad de Buenos Aires, Argentina and also with the CONICET, C1033AAJ, Ciudad de Buenos Aires, Argentina (e-mail: jose.lipovetzky@ieee.org; afaigon@fi.uba.ar).

Color versions of one or more of the figures in this paper are available online at <http://ieeexplore.ieee.org>.

Digital Object Identifier 10.1109/TNS.2014.2368361

more sensitive to radiation as the amount of electron-hole pairs generated increases and the capacitive coupling of the MOS structure decreases. All in all, the sensitivity increases approximately with the square of the oxide thickness [5]. However, in a standard CMOS fabrication process, it is not possible to control the thickness of the gate oxide and the sensitivity cannot be customized. Consequently, if a more sensitive dosimeter is needed, it has to be fabricated in a special process [6], increasing the dosimeter cost.

In [7], we proposed the fabrication of a high sensitive dosimeter by replacing the gate oxide in the MOSFET used as ionizing radiation sensor with the field oxide (FOX-FET) in a standard CMOS process. Field oxides are much thicker than standard gate oxides in the process, making the FOX-FET a much more sensitive dosimeter. Nevertheless, even though the sensitivity is comparable with that of commercially accepted dosimeters, it may not be high enough for very low dose applications, such as X-ray diagnosis.

A drawback in MOS dosimetry is the temperature induced shifts in  $V_T$  which can lead to sensor misreadings [8]. Whereas this may not be inconvenient for high dose measurements, special care should be taken to mitigate this effect in a low dose environment. Different techniques were proposed for this purpose [9], [10], [11], [12]. One of them takes advantage of the different sensitivity of identical dosimeters biased with different gate bias during irradiation to cancel  $V_T$  shifts other than those induced by radiation [11].

Based on [11], we have proposed in [13] a differential measurement technique which successfully minimizes the temperature effects in the dosimetric signal as well as allows real time measurements. In spite of the fact that the temperature induced error is diminished, the radiation sensitivity of the sensing devices was not improved significantly, and the dosimeter is not yet appropriate for X-ray dosimetry or lower dose applications.

In this paper we propose the use of circuit embedded sensors with the aim of getting sensitivity amplification as well as temperature induced error compensation, with CMOS compatible sensors and circuits. Different MOS based dosimeters have already been proposed in recent years [12], [14], [15], but without sensitivity amplification.

## II. DIFFERENTIAL MOS DOSIMETER WITH SENSITIVITY AMPLIFICATION

The circuit here presented was design with three main purposes: CMOS compatibility, sensitivity amplification, and

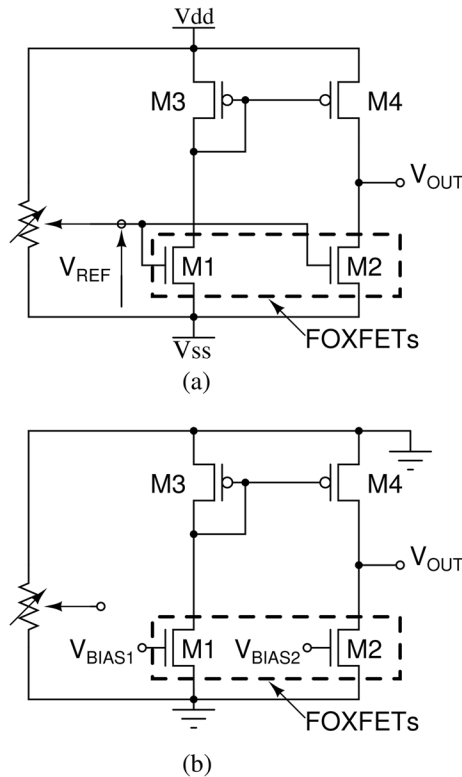


Fig. 1. Circuit schematic for the proposed sensor. In (a) the circuit is connected in “reading mode,” and in (b) the circuit is connected in “biasing mode.”

temperature induced error compensation. For CMOS compatibility, the sensors chosen are n-channel field oxide MOSFETs (FOXFETs) as in [7]. To achieve error minimization, differential sensing is proposed. Finally, as MOSFETs are inherently transconductance amplifiers, the shifts in  $V_T$  of the FOXFETs will affect the drain current if  $V_{GS}$  is kept constant.

Fig. 1 shows the proposed circuit following these guidelines. The circuit was named “unbalanced current sources” and switches between “reading mode,” corresponding to the schematic shown in Fig. 1(a), and “biasing mode,” Fig. 1(b), where every node in the circuit is grounded except for the gate of both sensors. The gate voltage of each FOXFET in “biasing mode” should be different in order to M1 and M2 to respond differently when exposed to radiation.

The circuit in Fig. 1(a) shows the dosimeter in “reading mode,” where two FOXFETs (M1 and M2) are loaded with a current mirror (M3 and M4) that forces the same drain current in both branches of the circuit. When M1 and M2 are matched,  $I_{D_{M1}} = I_{D_{M2}}$  (assuming no inherent offset) and the circuit remains steady with  $V_{out} = V_{G_p}$ , being  $V_{G_p}$  the gate voltage of the p-channel MOSFETs that comprises the current mirror. It is expected that when exposed to radiation, the threshold voltage of M1 and M2 will evolve differently due to the differential biasing, and mismatch will appear. To maximize this differential response, each sensor is biased independently in order for one of them to be in a PCB stage (positive bias), whereas the other one is in a radiation induced charge neutralization (RICN) stage (negative bias) [16].

### III. IMPLEMENTATION

In order to test the feasibility of the design, a discrete-level prototype circuit was built using different commercial and custom ICs.

The core of the circuit is the radiation sensitive pair. Two custom made FOXFETs [7] integrated in the same die were used. The FOXFETs are n-channel transistors, have an approximately 600 nm thick gate oxide, and a geometry  $W/L = 440 \mu\text{m}/25 \mu\text{m}$ , comprised of four fingers. The die is wire-bonded in a DIP40 package.

The p-type current mirror was implemented with the ALD1117 IC, a dual p-channel matched MOSFET array, which most important parameters are  $V_T = -0.7 \text{ V}$ ,  $k_p = \mu_p C_{OX} W/L = 0.4 \text{ mA/V}^2$ ,  $\lambda = 0.022 \text{ V}^{-1}$ . The ALD1117 response to radiation was studied, and a maximum sensitivity of  $5 \mu\text{V}/\text{rad}$  was observed, negligible in contrast with the FOXFET sensitivity.

In order to switch between “biasing mode” and “reading mode,” the MAX4533CPP IC was used, a quad analogue switches array. The circuit is supplied with a  $\pm 18 \text{ V}$  power supply, and the switches were commanded with a CMOS compatible digital signal from the Agilent 34970 data acquisition system, which is also in charge of providing the different gate bias ( $V_{BIAS1}$  and  $V_{BIAS2}$ ). The acquisition system is controlled by a computer and switches the circuit from “biasing” to “reading mode,” where it measures the output voltage and the gate voltages (from p-channel and n-channel transistors) every 11 seconds.

### IV. EXPERIMENTAL RESULTS

#### A. Circuit Response to $\gamma$ Radiation

The circuit was exposed to a  $^{60}\text{Co}$   $\gamma$ -source with dose rate of 37 rad/min to determine the sensor response to radiation. A pre-irradiation of the FOXFETs was needed in order to lower their  $V_T$  to approximately 3 V, making RICN possible.

Before irradiation, the FOXFETs were matched and  $V_{OUT} = V_{G_p} \approx 16 \text{ V}$ . During characterization of the circuit, M1 was biased with  $V_{BIAS1} = -10 \text{ V}$  for RICN and M2 with  $V_{BIAS2} = +10 \text{ V}$  for PCB. With this configuration, it was expected for  $I_{D_{M1}}$  to lower and for  $I_{D_{M2}}$  to increase, resulting in a reduction of  $V_{OUT}$ .

Fig. 2 shows the characterization for three different  $V_{REF}$ : 6.15 V, 9 V, and 15 V. In all cases, the output voltage dropped with radiation. In spite of the fact that the topology of the circuit suggests a high impedance output node [17], the response is not abrupt. For the drain currents involved, the ALD p-channel transistors in the active load present such a low output resistance to lower the impedance in the output node and the amplification. This relatively low amplification ensures that the random offset in the FOXFET sensing pair does not saturate the output signal.

As expected, with lower  $V_{REF}$  the sensitivity was higher as the currents in the circuit are lower, increasing the output resistance of all transistors. The response is nonlinear, showing the maximum sensitivity around  $V_{OUT} \approx -3 \text{ V}$  for every  $V_{REF}$  as shown in Fig. 3. The highest sensitivity measured

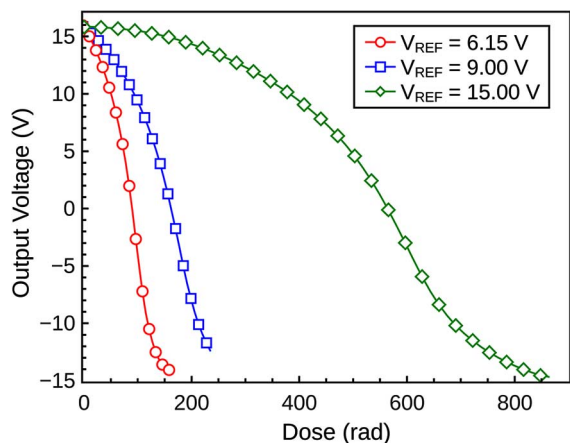


Fig. 2. Circuit response to dose for different  $V_{REF}$ . When the reference voltage is lower, the sensitivity increases as well as the the dose range decreases.

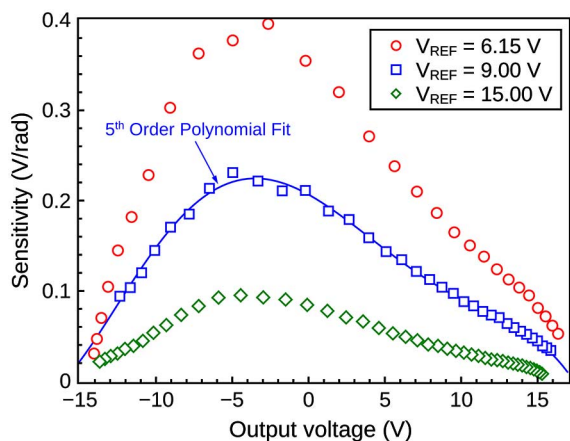


Fig. 3. Circuit sensitivity to radiation as a function of the output voltage for different  $V_{REF}$ . The sensitivity was calculated as the backward discrete derivative of the response curve in Fig. 2. For every reference voltage, a maximum sensitivity is achieved between  $-1$  V and  $-5$  V of  $V_o$ .

was  $0.4$  V/rad for  $V_{REF} = 6.15$  V. The output range is approximately  $-15$  V  $< V_{OUT} < 16$  V, where the upper limit is due to the p-channel MOSFETs from the ALD1117 leaving the saturation regime, whereas the lower limit is due to the FOXFETs leaving the saturation regime.

### B. Circuit Response to X-Rays

The circuit was then tested for X-ray diagnose dosimetry. It was irradiated with an X-ray generator for radiology imaging, *Pimax 30–50 kVA, 125 kV*, and the dose was recorded using a *PTW Freiburg UNIDOS E* dosimeter with ionization chamber *SFD 34060*. The tube was set with a  $15$  cm  $\times$   $15$  cm field and the sensor was placed in the stretcher,  $100$  cm away from the ray source. The reference voltage was set to  $9.00$  V, and the FOXFET sensing pair was biased with  $V_{BIAS1} = -10$  V and  $V_{BIAS2} = 10$  V during “biasing mode.” The electronic set-up and the acquisition system was the same as for the  $\gamma$  calibration.

The output voltage was recorded while exposed to different X-ray shots corresponding to different combinations of charge and energy. A time chart that exemplifies this experiment is shown in Fig. 4, where different shots with different beam energies were measured. It can be seen that with higher energies,

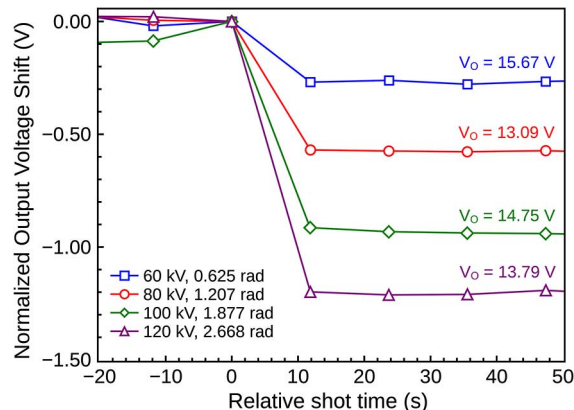


Fig. 4. Time chart for the output voltage shift for different X-ray shots at different energies. The charge was set to  $200$  mAs for every shot.

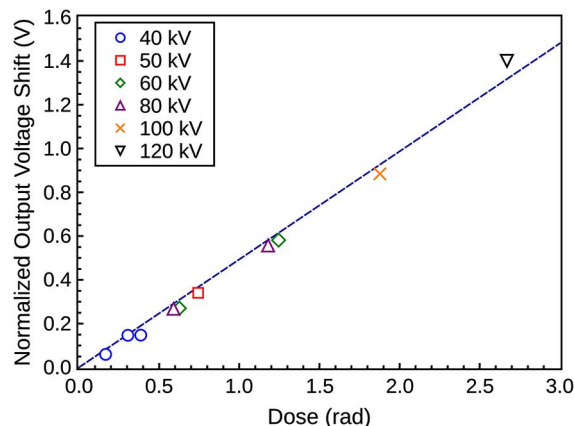


Fig. 5. Calibration of the circuit to X-ray beams. Markers are measurements and the dashed line shows the linear fit yielding a sensitivity of  $0.49$  mV/rad.

the dose delivered increases and the sensor output shifts accordingly.

As the sensor has a nonlinear behavior, in order to normalize the dosimetric signal to the highest sensitivity, a 5th order polynomial correction of the output voltage difference was performed. The calibration polynomial was obtained from the sensor response to  $\gamma$  radiation and is plotted along with the measurements in Fig. 3. After correction, the calibration curve for X-rays in Fig. 5 was obtained. The figure shows the calibration with the measured dose. Different colors in the plotted markers indicate the energy of the beam. Measurements show a normalized sensitivity of approximately  $0.49$  V/rad, obtained from the slope of a linear fit of the measurements.

### C. Temperature Compensation

To test temperature compensation, the circuit was heated up to  $70$   $^{\circ}$ C with no radiation field applied, and the output voltage was recorded. The reference voltage was set to  $V_{REF} = 6.15$  V. The experiment was carried out in the maximum sensitivity condition, i.e.  $V_{OUT} \approx -1$  V, and repeated in the maximum matching condition, i.e.  $V_{OUT} = V_{Gp} \approx 16$  V.

As expected, the temperature effects in the FOXFETs were better compensated when the devices were matched, rather than in the highest sensitivity condition. Fig. 6 shows the shifts in  $V_{OUT}$  with temperature, exhibiting a temperature sensitivity of

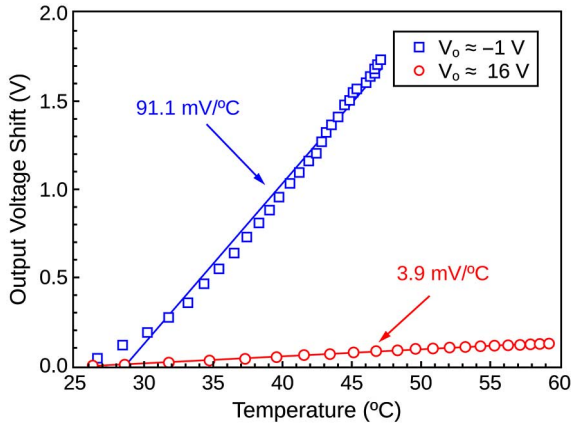


Fig. 6. Circuit response to temperature for different steady state  $V_o$ . When the FOXFETs are mismatched, the temperature sensitivity increases, whereas when they are matched, a lower temperature sensitivity is observed.

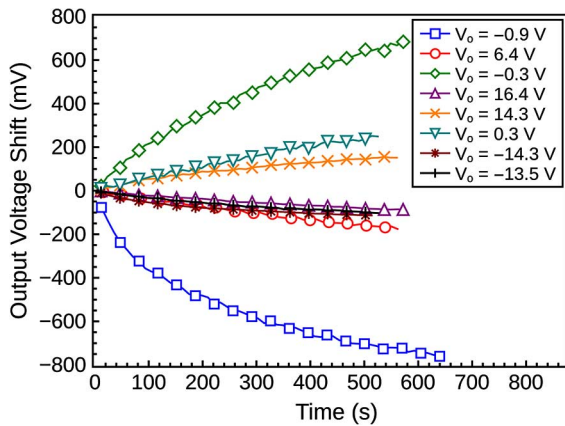


Fig. 7. Shift in the output voltage as a function of the post-irradiation time.

about  $3.9 \text{ mV}/^\circ\text{C}$  when the devices were matched, and a sensitivity of about  $91 \text{ mV}/^\circ\text{C}$  when the radiation sensitivity is maximized. Taking into account the radiation sensitivity amplification in each scenario, this means that when the sensitivity is the highest, the dose error induced by temperature, the *temperature error factor* (TEF) [13], is about  $230 \text{ mrad}/^\circ\text{C}$ , whereas when the devices are matched, the error is approximately  $78 \text{ mrad}/^\circ\text{C}$ .

#### D. Fading and Noise Performance

In order to evaluate the noise performance and fading of the circuit, short-time sessions of radiation were delivered to the sensor. After the radiation pulse,  $V_{OUT}$  was tracked for 9 min.

Fig. 7 shows the fading characteristics at every  $V_{OUT}$  studied. The maximum fading registered was observed around  $-1 \text{ V}$  showing negative shifts in the output voltage of approximately  $750 \text{ mV}$  in 10 min.

Knowing the fading characteristics, this temporal behavior was subtracted from the dosimetric signal in order to unveil the noise signal. For each output voltage, the RMS noise voltage was calculated from the noise signal. The process described in the preceding paragraphs was repeated for a higher  $V_{REF}$ , expecting lower noise power due to a higher drain current in the

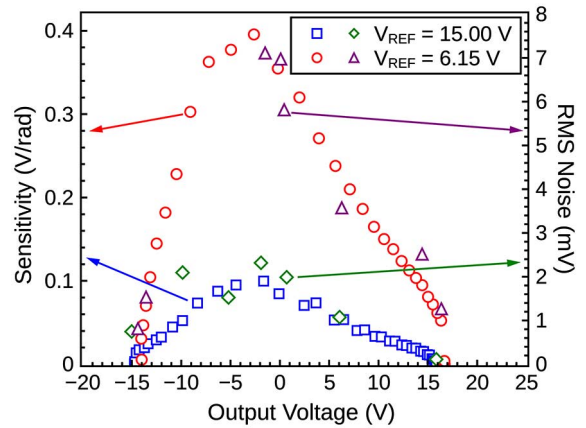


Fig. 8. RMS noise of the dosimetric signal (right axes) and sensitivity to radiation (left axes) to output voltage. Both curves maintain a similar shape showing that the noise equivalent dose of  $19 \text{ mrad}$  remains constant regardless the reference voltage or the steady state output voltage.

FOXFETs. The results are plotted in Fig. 8 along with the radiation sensitivity for each biasing condition. In the figure it can be observed that effectively the noise is lower with a higher  $V_{REF}$ , but also the radiation sensitivity decreases. Adjusting both ordinate axes, it can be observed that the noise and the sensitivity have the same dependence with the output voltage. Hence, there is no expectation for an optimal operation point as regards signal-to-noise ratio.

## V. DISCUSSION

In this paper a new differential radiation sensor based on n-channel FOXFETs was presented and characterized. The output voltage of the new sensor circuit is related to the drain current difference that appears when the FOXFET sensing pair is mismatched due to radiation. The characterization was based on response to radiation, temperature effects mitigation, fading, and signal-to-noise ratio.

#### A. Response to Radiation

The sensor presents a nonlinear response to radiation and a limited output range. For the sensor to work properly, all transistors must be in the saturation regime. The output characteristics of the sensor is similar to that of the differential amplifier [17]. The output voltage upper boundary is  $V_{dd} - |V_{DS,p_{sat}}|$ , when the p-MOSFET from the current mirror goes to saturation, and the lower boundary is  $V_{DS,n_{sat}} - |V_{ss}|$ , when the FOXFET goes to saturation regime. This means that the output range is limited by the power supply. The nonlinearity can be explained with the small signal model. The change in the output voltage is  $\Delta V_{OUT} = g_m \times R_{OUT} \times \Delta V_T$  and both parameters, the transconductance and the output resistance, are dependent on the drain currents. As the drain currents change with radiation, so do these parameters. Moreover, the transconductance of each FOXFET is involved in the circuit functionality and, as the drain current of each FOXFET varies differently, so will their transconductance. The same apply for the output resistance of each transistor in the circuit. This complex interaction of parameters leads to the observed nonlinear behavior.

The sensitivity of the circuit to radiation depends on the quiescent point, and a maximum sensitivity is achieved around  $V_{OUT} = -3$  V. When the reference voltage during “reading mode” is set to  $V_{REF} = 6.15$  V, we measured the highest sensitivity to  $\gamma$  radiation of 0.4 V/rad.

In [7] we tested the FOXFET dosimeter with the standard reading method and we were able to achieve a 4.4 mV/rad sensitivity with a gate bias of 12 V. This means that with this new circuit we were able to obtain a  $91\times$  gain. This gain may be augmented if special care is taken when choosing all parameters involved in the functionality of the sensor, such as  $V_{REF}$ ,  $V_{BIAS1/2}$ , and the pre-irradiated initial  $V_T$ .

The radiation sensitivity amplification showed to be enough for X-ray dosimetry. The sensor was tested with a diagnosis X-ray machine and calibrated with a ionizing chamber. The calibration showed a sensitivity of 0.4 V/rad with a  $V_{REF} = 9.00$  V, almost twice as high as for  $\gamma$  radiation with the same  $V_{REF}$ . This difference in sensitivities is already known and is attributed to the dose enhancement effect [18].

### B. Temperature Induced Error

As regards temperature variations, as expected, the mismatch induced in order to enhance the sensor sensitivity impoverishes the temperature compensation. When a 0.4 V/rad sensitivity to radiation is achieved, a 91 mV/ $^{\circ}$ C sensitivity to temperature is obtained. We showed in [13] that when the FOXFET is used as a single MOSFET dosimeter with the standard measurement technique, the temperature sensitivity was 2.6 mV/ $^{\circ}$ C, much lower than the circuit presented here. Nevertheless, the gain in radiation sensitivity is higher than the one for temperature, hence the TEF improves. Whereas the TEF in the standard FOXFET dosimeter is 0.59 rad/ $^{\circ}$ C, the TEF in the circuit here proposed is only 0.23 rad/ $^{\circ}$ C, less than half.

Despite this improvement compared to the standard MOS dosimeter, temperature error compensation is not as good as the one obtained in [13]. The differential reading technique presented in that work showed a TEF as low as 27 mrad/ $^{\circ}$ C, almost ten times better than the amplified dosimeter. This difference is easy to explain and shows the major drawback of this implementation. In order to achieve radiation sensitivity amplification, the FOXFETs should be firstly mismatched, and secondly biased with different drain-source voltage and different drain current. This means that at every moment, the FOXFETs are working in different conditions and their response to any stimulus will be different.

Nevertheless, if the sensor is used in applications such as X-ray diagnose dosimetry, the measuring time will be a fraction of second. In such a short time, the temperature in the sensor is unlikely to change more than 0.1 $^{\circ}$ C, considering normal operation conditions, and the dose error induced by temperature will be lower than 23 mrad and probably could be neglected.

### C. Fading, Noise, and Minimum Resolvable Dose

The circuit presented fading characteristics, i.e., the output voltage suffers a monotonic variation when not exposed to radiation. The worst case fading (10 min) is approximately 80 mV min measured near the highest amplification conditions. For the applications and the real-time measurement technique presented

here, the fading is not a complication as the measurements are taken instantaneously during the irradiation session.

The noise was also studied. It was observed that the *noise equivalent dose* (NED) [13], the ratio between the noise voltage and the radiation sensitivity, of the sensor was independent from the quiescent point and it is about 19 mrad. When the same study was carried out for the standard FOXFET dosimeter, a NED equal to 12 mrad was measured. This impoverishment in the sensor resolution can be explained if we consider that each FOXFET contributes to the noise in the output of the circuit, meaning that the noise from each transistor is added, and is in turn amplified. A similar result was obtained in [13] as the technique presented in that work also involved two FOXFET devices in the measurement.

### D. CMOS Integrated Circuit Manufacturability

Finally, we will discuss the possibility to transfer the design to an integrated circuit. In this case, the core of the sensor are the FOXFETs, which were already fabricated in a 0.5  $\mu$ m CMOS process. The difficulty in order to integrate the differential amplification is that the FOXFETs have a very high initial threshold voltage, approximately 20 V. As a pre-irradiation is required in order to be able to apply RICN, this  $V_T$  will be lowered in this procedure. CMOS fabrication processes usually offer *high voltage devices* which allow operation with 12 V, 18 V, or even higher voltages. With a cautious design and the pre-irradiation procedure above mentioned, it is expected to achieve a fully operational dosimeter like the one presented in this paper monolithically integrated in a CMOS process. This work is in progress.

## VI. CONCLUSIONS

In conclusion, a MOS based dosimeter with sensitivity amplification was designed and the sensor was successfully characterized to be used for X-ray dosimetry. The sensitivity to  $\gamma$  radiation was amplified up to 91 times with respect to the *single FOXFET dosimeter*[7], and with proper design even a greater amplification can be obtained.

We showed that the temperature induced error was reduced by half compared to the single FOXFET approach. Nevertheless, the temperature compensation was not as good as we expected, and the reading technique we proposed in [13] showed better results, but in that case there were no amplification benefits. It is being investigated the possibility of merging both techniques in order to meet both requirements.

The nonlinearity of the sensor response is also not desirable and the amplification is difficult to control due to variability of the electrical parameters of the devices in the sensor. The amplification and dynamic output range is highly dependent on the output resistance which may not be easily controlled when fabricated in an integrated circuit.

All things considered, it is concluded that for future designs the best approach for a robust sensor is to use a feedback circuit. This will allow to control the stability, the closed loop gain for radiation sensitivity, and will enhance the linearity of the output voltage. Also, future work will be aimed to improve the temperature compensation and to lower the noise of the circuit.

## ACKNOWLEDGMENT

The authors want to thank the Marie Curie Hospital for the access to irradiation facilities and Susana Blanco for her assistance in dosimetry.

## REFERENCES

- [1] A. Holmes-Siedle, "The space-charge dosimeter: General principles of a new method of radiation detection," *Nuclear Instruments and Methods*, vol. 121, no. 1, pp. 169–179, 1974.
- [2] G. Sarrabayrouse and S. Siskos, "Radiation dose measurement using mosfets," *Instrumentation and Measurement Magazine*, vol. 1, no. 2, pp. 26–34, 1998.
- [3] T. R. Oldham and F. B. McLean, "Total ionizing dose effects in MOS oxides and devices," *IEEE Trans. Nucl. Sci.*, vol. 50, no. 3, pp. 483–499, 2003.
- [4] J. R. Schwank, M. R. Shaneyfelt, D. M. Fleetwood, J. A. Felix, P. E. Dodd, P. Paillet, and V. Ferlet-Cavrois, "Radiation effects in MOS oxides," *IEEE Trans. Nucl. Sci.*, vol. 55, no. 4, pp. 1833–1853, Aug. 2008.
- [5] N. S. Saks, M. G. Ancona, and J. A. Modolo, "Radiation effects in MOS capacitors with very thin oxides at 80 K," *IEEE Trans. Nucl. Sci.*, vol. 31, no. 6, pp. 1249–1255, 1984.
- [6] G. Sarrabayrouse and S. Siskos, "Low dose measurement with thick gate oxide mosfets," *Radiation Physics and Chemistry*, vol. 81, no. 3, pp. 339–344, 2012.
- [7] J. Lipovetzky, M. A. García-Inza, S. Carbonetto, M. J. Carra, E. Redin, L. Sambuco Salomone, and A. Faigon, "Field oxide n-channel mos dosimeters fabricated in cmos processes," *IEEE Trans. Nucl. Sci.*, vol. 60, no. 6, pp. 4683–4691, 2013.
- [8] A. Haran, A. Jaksic, N. Refaeli, A. Eliyahu, D. David, and J. Barak, "Temperature effects and long term fading of implanted and unimplanted gate oxide RADFETs," *IEEE Trans. Nucl. Sci.*, vol. 51, no. 5, pp. 2917–2921, 2004.
- [9] S. H. Carbonetto, M. A. García-Inza, J. Lipovetzky, E. G. Redin, L. Sambuco Salomone, and A. Faigon, "Zero temperature coefficient bias in MOS devices. dependence on interface traps density, application to MOS dosimetry," *IEEE Trans. Nucl. Sci.*, vol. 58, no. 6, pp. 3348–3353, 2011.
- [10] J. Lipovetzky, E. G. Redin, M. A. García-Inza, S. Carbonetto, and A. Faigon, "Reducing measurement uncertainties using bias cycled measurement in MOS dosimetry at different temperatures," *IEEE Trans. Nucl. Sci.*, vol. 57, no. 2, pp. 848–853, 2010.
- [11] M. Soubra, J. Cygler, and G. Mackay, "Evaluation of a dual bias dual metal oxide-silicon semiconductor field effect transistor detector as radiation dosimeter," *Med. Phys.*, vol. 21, no. 4, pp. 567–572, 1994.
- [12] N. G. Tarr, K. Shortt, Y. Wang, and I. Thomson, "A sensitive, temperature-compensated, zero-bias floating gate MOSFET dosimeter," *IEEE Trans. Nucl. Sci.*, vol. 51, no. 3, pp. 1277–1282, 2004.
- [13] M. García-Inza, S. Carbonetto, J. Lipovetzky, M. J. Carra, L. Sambuco Salomone, E. G. Redin, and A. Faigon, "Switched bias differential MOSFET dosimeter," *IEEE Trans. Nucl. Sci.*, vol. 61, no. 3, pp. 1407–1413, Jun. 2014.
- [14] A. Shamim, M. Arsalan, L. Roy, M. Shams, and G. Tarr, "Wireless dosimeter: System-on-chip versus system-in-package for biomedical and space applications," *IEEE trans. Circuits and Systems II: Express Briefs*, vol. 55, no. 7, pp. 643–647, 2008.
- [15] E. García-Moreno, E. Isern, M. Roca, R. Picos, J. Font, J. Cesari, and A. Pineda, "Floating gate CMOS dosimeter with frequency output," *IEEE Trans. Nucl. Sci.*, vol. 59, no. 2, pp. 373–378, 2012.
- [16] D. M. Fleetwood, "Radiation induced charge neutralization and interface trap buildup in metal oxide semiconductor devices," *J. Applied Physics*, vol. 67, no. 1, pp. 580–583, 1990.
- [17] P. E. Allen and D. R. Holberg, *CMOS Analog Circuit Design*. : Oxford University Press, 2012.
- [18] A. B. Rosenfeld, M. G. Carolan, G. I. Kaplan, B. J. Allen, and V. I. Khivrich, "Mosfet dosimeters: The role of encapsulation on dosimetric characteristics in mixed gamma-neutron and megavoltage X-ray fields," *IEEE Trans. Nucl. Sci.*, vol. 42, no. 6, pp. 1870–1877, 1995.